



TecnoLógicas
ISSN-p 0123-7799
ISSN-e 2256-5337
Vol. 23, No. 48, pp. 163-179
Mayo-agosto de 2020

Artículo de Investigación/Research Article

TecnoLógicas

Reliability Analysis of Bored-pile Wall Stability Considering Parameter Uncertainties

Análisis por confiabilidad de la estabilidad de muros de pilas excavadas considerando las incertidumbres de los parámetros

Álvaro J. Mattos ¹,
Roberto J. Marín ²

Recibido: 17 de julio de 2019
Aceptado: 17 de abril de 2020

Cómo citar / How to cite

Á. J. Mattos, R. J. Marín, "Reliability Analysis of Bored-pile Wall Stability Considering Parameter Uncertainties", *TecnoLógicas*, vol. 23, no. 48, pp. 163-179, 2020. <https://doi.org/10.22430/22565337.1433>

© Instituto Tecnológico Metropolitano
Este trabajo está licenciado bajo una
Licencia Internacional Creative
Commons Atribución (CC BY-NC-SA)



- ¹ MSc. in Engineering, Geo-Research International (GeoR), Environmental School, Faculty of Engineering, University of Antioquia, Medellín-Colombia, alvaro.mattos@udea.edu.co of Antioquia, Medellín-Colombia, alvaro.mattos@udea.edu.co
- ² MSc. in Engineering, Landslide Scientific Assessment (LandScient), Infrastructure Investigation Group (GII), Environmental School, Faculty of Engineering, University of Antioquia, Medellín-Colombia, rjose.marin@udea.edu.co

Abstract

In geotechnical engineering, bored-pile wall stability is evaluated using deterministic design methods based on safety factors to establish a margin against failure. In recent years, reliability-based design methods have been adopted to include uncertainty in the assessment of bored-pile wall stability as well as in the calculation of the feasible embedment depth of the walls. In this study, an expanded reliability-based design approach, along with finite element analysis, was applied to conduct parametric analyses of bored-pile wall stability. In serviceability limit state design framework, the results indicate that cohesion and groundwater level are factors that significantly affect bored-pile wall stability. Moreover, high variability in the cohesion range causes great uncertainty to determine the embedment depth of bored-pile wall. The feasible embedment depth can reach 4 times the free height considering the maximum coefficient of variation (50 %) of the cohesion. In turn, when the groundwater level is located at the retained ground surface, the horizontal displacement of the upper end of the wall reaches 15.2 mm, i.e., 0.0038 times the free height of the wall, for which the soil mobilizes active earth pressures. It was also found that the resolution of probabilistic results is highly influenced by the number of iterations in Monte Carlo simulations.

Keywords

Bored-pile wall, embedment depth, reliability-based design, Monte Carlo simulation, finite element analysis.

Resumen

En ingeniería geotécnica, la estabilidad de muros de pilas excavadas es evaluada mediante métodos de diseño determinísticos que se basan en el uso de factores de seguridad para establecer un margen para la falla. En los últimos años, se han adoptado métodos de diseño basados en la confiabilidad para involucrar la incertidumbre en la evaluación de la estabilidad de los muros, así como para el cálculo de la profundidad de empotramiento factible para los muros. En este estudio, se aplica un enfoque de diseño basado en la confiabilidad ampliada para desarrollar análisis paramétricos de la estabilidad de un muro de pilas excavadas, junto con un análisis de elementos finitos. En el marco del diseño por estado límite de servicio, los resultados indican que la cohesión del suelo y el nivel freático son factores que afectan significativamente la estabilidad del muro. Una alta variabilidad en el rango de cohesión causa una gran variabilidad en la incertidumbre para determinar la profundidad de empotramiento del muro. La profundidad de empotramiento factible puede alcanzar 4 veces la altura libre considerando el coeficiente de variación máximo (50 %) de la cohesión del suelo. Por otro lado, cuando el nivel freático se ubica en la superficie del terreno retenido, el desplazamiento horizontal del extremo superior del muro alcanza 15.2 mm, equivalente a 0.0038 veces la altura libre del muro, para el cual el suelo alcanza a movilizar los empujes activos. También se encontró que la resolución de los resultados probabilísticos está altamente influenciada por el número de iteraciones en las simulaciones de Monte Carlo.

Palabras clave

Muro de pilas excavadas, profundidad de empotramiento, diseño basado en la confiabilidad, simulación de Montecarlo, análisis de elementos finitos.

1. INTRODUCTION

The geotechnical analysis of bored-pile wall stability usually involves deterministic design methods based on the use of a target global factor of safety to establish a margin against failure [1].

Nevertheless, in recent years, there has been a noticeable shift from deterministic to reliability-based design methods, which involve uncertainty analysis and reliability assessment for wall embedment depth calculation [2], [3]. The latter type of methods offer more flexibility in terms of adjusting design parameters to reach or exceed a specific safety level (e.g., reliability index or failure probability) [4].

Additionally, including a quantitative analysis of uncertainties in geotechnical design procedures in a consistent way is essential to obtain adequate designs of geotechnical structures in geological/geotechnical engineering [5].

These methodologies have been applied to geotechnical analyses by means of the First-Order Second-Moment method (FOSM) [6], [7], First-Order Reliability Method (FORM) [8], Second-Order Reliability Method (SORM) [9], and Monte Carlo simulation (MCS) [10]–[12].

The application of reliability-based design methods relies on the knowledge of the statistical data of soil design parameters that have a significant effect on the stability of earth retaining structures [13], [14]. In an uncertainty analysis framework, uncertain engineering quantities (i.e., soil strength) are modeled by random variables through stochastic models (e.g., FORM, Monte Carlo simulation, etc.) to obtain, as a result, a relationship between a model outcome (e.g., embedment depth) and either the probability of failure or the reliability index of the geotechnical system [15].

Reliability-based designs require the definition of probability density functions of geotechnical properties and knowledge of soil spatial variability [16].

In turn, in reliability risk assessment, a feasible model outcome (e.g., feasible embedment depth) is calculated based on a target probability of failure p_T (or a target reliability index β_T), which is selected according to design code specifications [17].

Those target probabilities of failure proposed by design codes (mainly foundation codes) range from $p_T = 4.7 \times 10^{-3}$ to $p_T = 4.8 \times 10^{-7}$, and their use in reliability analyses is mainly justified by the consequences and nature of structure failures, economic losses, and social inconveniences (e.g., loss of human lives) [14], [18].

Several geotechnical design codes, such as ISO2394 [19] and Eurocode-7 [20] have recommend the use of reliability-based design methods to conduct parametric studies of design variables involved in the stability of retaining walls [21], [22] since, from a geotechnical perspective, the role of reliability calculations consists in applying a parametric study to reveal the significance of the variation of lead variables; in particular, a careful assessment of the worst credible values of parameters [23].

In this study, an expanded reliability-based design is developed to conduct parametric studies into bored-pile wall stability considering geotechnical parameters distributed as random variables. In addition, finite element calculations, in combination with serviceability limit state design framework (based on geotechnical design standards), were used as a complementary methodology to deal with the variations in the geotechnical parameters of the soil-structure interaction analysis.

2. METHODOLOGY

2.1 Overview of the bored-pile wall design procedure

Currently, a common design practice for cantilever bored-pile walls is based on the limit equilibrium approach [24].

Several limit equilibrium methods have been applied to determine the wall embedment depth in granular soils (e.g., [25]). NSR-10 [1] recommends the use of classical design methods; therefore, the simplified method [26] may be applied to calculate the wall embedment depth required to ensure the lateral earth pressure balance by considering the moment equilibrium about the lower end of the wall. The embedment depth of the wall is calculated by Murthy [27] as (1).

where FS is the factor of safety of the wall stability, which defines the domain of failure of the wall as $FS < 1$; K_a and K_p , earth pressure coefficients for active and passive condition, respectively; H , the free height of the wall; and D , the embedment depth of the wall.

Earth pressures behind and in front of the wall are calculated by (2) and (3).

where σ'_v represents effective vertical stress and $\sigma'_{a,p}$ is the effective horizontal stress for either active or passive condition, γ is the unit soil weight, z is the depth to any point below the ground surface, $K_{a,p}$ is the earth pressure coefficient for either

active or passive condition; and u is the pore pressure of the soil, which is calculated by (4).

Where γ_w is the unit weight of water and h_w is the difference between z (below groundwater level) and the groundwater level.

As a complement, the analytical solution of Mazindrani and Ganjali [28] (5) can be used to evaluate the earth pressure coefficients when dealing with retaining walls with cohesive backfill soil and an inclined surface.

Where α is the slope angle of the backfill soil surface; c' , the effective cohesion; and ϕ' , the effective angle of internal friction of the soil.

2.2 Reliability and numerical modeling procedure

2.2.1 Expanded reliability-based design

The expanded reliability-based design (RBD^E) approach refers to a reliability analysis of a system in which a set of system design parameters are virtually considered as uncertain, with probability distributions specified by the user, for design exploration purposes [17].

For geotechnical structures, the design process is formulated as an expanded reliability problem in which Monte Carlo simulations are used (e.g., [29], [30]).

$$FS = \frac{(K_p - K_a)D^3}{3HD(H + D)K_a}, \quad (1)$$

$$\sigma'_v = \gamma z - u \quad (2)$$

$$\sigma'_{a,p} = K_{a,p}\sigma'_v \mp 2c'\sqrt{K_{a,p}} \quad (3)$$

$$u = (\gamma - \gamma_w)h_w \quad (4)$$

$$k_p, k_a = \frac{1}{\cos^2 \phi'} \left\{ 2\cos^2 \alpha + 2 \left(\frac{c'}{\gamma z} \right) \cos \phi' \sin \phi' \pm \sqrt{4\cos^2 \alpha (\cos^2 \alpha - \cos^2 \phi') + 4 \left(\frac{c'}{\gamma z} \right)^2 \cos^2 \phi' + 8 \left(\frac{c'}{\gamma z} \right) \cos^2 \alpha \sin \phi' \cos \phi'} \right\} - 1 \quad (5)$$

Similar to the reliability-based design of drilled shafts [31], RBD^E's application to bored-pile wall analysis consists in considering basic design parameters, such as the normalized embedment depth (D/H), the slope angle of the backfill soil surface (α), and normalized groundwater level (h_1/H), as discrete uniform random variables. Then, the design process becomes one in which the probability of failure is developed for various combinations of D/H and the other design parameters [i.e., the conditional probability $p(\text{Failure} | D/H, \alpha, h_1/H)$], and are compared with a target probability of failure on the service limit state p_T^{SLS} .

Feasible designs are those with $p(\text{Failure} | D/H, \alpha, h_1/H) \leq p_T^{SLS}$ [14].

Using Bayes' theorem, the conditional probability $p(\text{Failure} | D/H, \alpha, h_1/H)$ is given by (6).

where $p(D/H, \alpha, h_1/H | \text{Failure})$ is a conditional joint probability of D/H , α , and h_1/H given the occurrence of failure.

Since D/H , α , and h_1/H are independent discrete uniform random variables, $p(D/H, \alpha, h_1/H)$, in (6), is expressed as (7).

where $n_{D/H}$, n_α , and $n_{h_1/H}$ = number of possible discrete values for each design parameter. The quantities $p(D/H, \alpha, h_1/H | \text{Failure})$ and p_f in (7) are estimated using a single run of a MCS. To calculate the minimum number of iterations to run in Monte Carlo simulations, (8) is applied

$$p(\text{Failure} | D/H, \alpha, h_1/H) = \frac{p(D/H, \alpha, h_1/H | \text{Failure})}{p(D/H, \alpha, h_1/H)} p_f \quad (6)$$

$$p(D/H, \alpha, h_1/H) = \frac{1}{n_{D/H} n_\alpha n_{h_1/H}} \quad (7)$$

based on examples given by Ang and Tang [32] and Wang and Cao [17].

where n_{\min} is the minimum number of iterations; p_T , the target probability of failure ($p_T=0.001$ according to Wang [3]); and COV_T , the target coefficient of variation for the failure probability estimated from Monte Carlo simulations ($COV_T=30\%$ according to Wang & Cao [17]).

2.2.2 Monte Carlo simulation

A Monte Carlo simulation is a stochastic method that creates models of possible outcomes by substituting random values of random variables (e.g., soil parameters) with their probability functions [33].

In this study, repeated random samples of uncertainty variables were generated from their probability density function using MS Excel and the @Risk add-in.

The Latin Hypercubic sampling technique was implemented for efficient sampling. The outcomes of the Monte Carlo simulation were statistically analyzed to estimate p_f and $p(D/H, \alpha, h_1/H | \text{Failure})$ as [14].

where, in (9) and (10), n is the total number of simulation samples; n_f , the number of simulation samples where failure occurs; and n_1 , the number of simulation samples where failure and a specific set of values of the uncertainty variable (i.e., D/H , α , and h_1/H) occur simultaneously.

$$n_{min} = \frac{((1/p_T) - 1) n_{D/H} n_{\alpha} n_{h_1/H}}{(COV_T)^2} \quad (8)$$

$$p_f = \frac{n_f}{n}, \quad (9)$$

$$p(D/H, \alpha, h_1/H | Failure) = \frac{n_1}{n_f}, \quad (10)$$

2.2.3 Case study

A generic geotechnical engineering problem published in the CIRIA Report C760 [34] involves the design of a cantilever bored-pile wall embedded in a $c' - \phi'$ soil under drained conditions. The retaining wall is a hard/hard secant bored-pile wall (0.75-m pile diameters at 0.65-m spacing) with $EI = 469,000 \text{ kNm}^2/\text{m}$, $EA = 8,660,000 \text{ kN/m}$, and $\gamma_{\text{concrete}} = 24 \text{ kN/m}^3$, where E is the modulus of elasticity of the pile; I , the moment of inertia; and A , the pile cross-section. The wall is subjected to a 10-kPa surcharge over the backfill soil, and the groundwater level is located 1 m below the backfill soil surface and 1 m below dredge level in front of the wall, as is shown in Fig. 1. The key parameter to determine in the geotechnical design is the wall embedment depth considering the properties of the soil shown in Table 1.

2.2.4 Model parametrization for reliability-based design

To perform a parametric analysis of the uncertainty variables in bored-pile wall design, several values of D , α , and h_1 are assumed for the reliability analysis according to the case study

problem. Table 2 shows the proposed values and probability distribution functions (PDFs) of the geotechnical variables. Both the PDFs and the coefficients of variation (COV) of the shear resistance parameters of the soil shown in Table 2 are commonly used to model soil uncertainty in virtual environments [35], [36]. The slope angle of the backfill soil surface, groundwater level on the active side of the wall, and embedment depth are defined as uniform discrete random variables according to reliability-based design concepts. The parameter $\Delta D = 0.25 \text{ m}$ indicates that, after the depth embedment range ($4 \text{ m} \leq D \leq 20 \text{ m}$), all the values are considered, each one separated by $D = 0.25 \text{ m}$; that is, $D \in \theta$, where $\theta = \{4 \text{ m}, 4.25 \text{ m}, 4.5 \text{ m}, \dots, 19.5 \text{ m}, 19.75 \text{ m}, 20 \text{ m}\}$.

Fig. 2 shows a diagram of the model parametrization for the reliability-based design, where the distance h_1 represents the groundwater level measured from the backfill soil surface, and h_2 denotes the distance from h_1 to the dredge level on the passive side. The groundwater level in front of the wall is assumed at the excavated surface level.

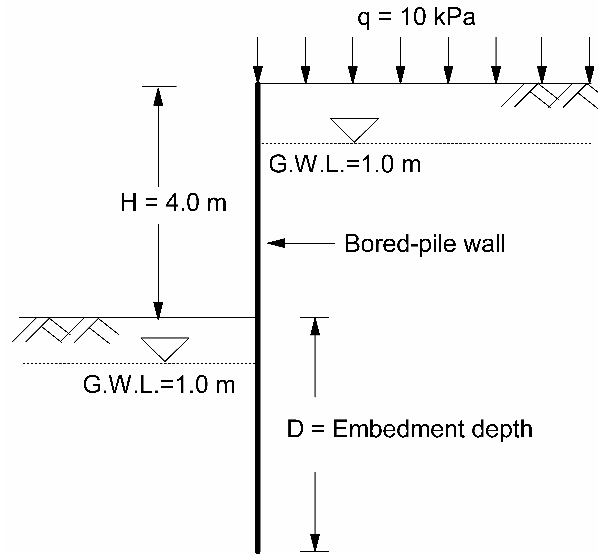


Fig. 1. Cantilever bored-pile wall design adapted from CIRIA Report C760. Source:[34].

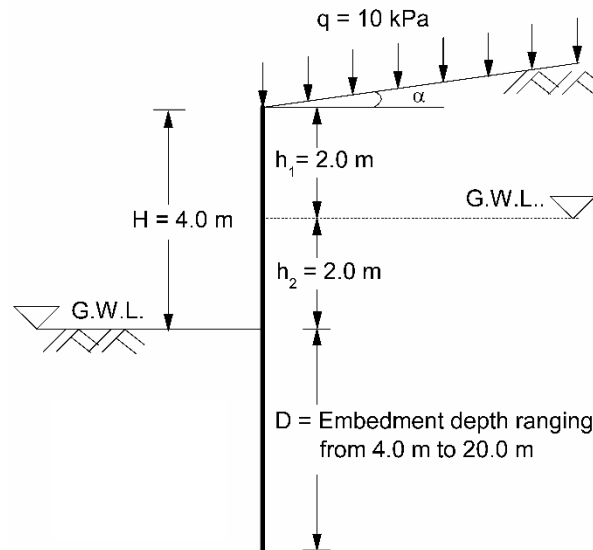


Fig. 2. Modified cantilever bored-pile wall design, modified from CIRIA Report C760. Source: [34].

Table 1. Properties of the backfill soil and the soil in front of the wall. Source: [34].

Property	Soil
Unit weight, γ	20 (kN/m ³)
Friction angle, ϕ'	25 (°)
Cohesion, c'	5 (kPa)
Modulus of elasticity, E'_s	48,000 (kPa)
Poisson's ratio, ν'	0.25
Soil/wall friction, δ/ϕ'	1.0
Permeability, k	1×10^{-9} (m/s)

Table 2. Uncertainty model for reliability analysis
 Source: Created by the authors.

Parameters	PDF	Variable type	Mean	COV
Friction angle, ϕ'	Normal	Continuous	25°	5 %, 10 %, 15 %
Cohesion, c'	Normal	Continuous	5 kPa	10 %, 30 %, 50 %
Unit weight, γ	Deterministic	-	20 kN/m ³	
Surcharge, q	Deterministic	-	10 kPa	
Free height, H	Deterministic	-	4 m	
Slope angle, α	Uniform	Discrete	$\alpha = 0^\circ, \alpha = 5^\circ, \alpha = 10^\circ, \alpha = 15^\circ$	
G.W.L. (Active side), h_1	Uniform	Discrete	$h_1 = 0 \text{ m}, h_1 = 2 \text{ m}, h_1 = 4 \text{ m}$	
G.W.L. (Passive side)	Deterministic	-	0 m	
Depth embedment, D	Uniform	Discrete	Min: 4 m; Max: 20 m; ΔD : 0.25 m	

Because of the above, the number of iterations to run in the Monte Carlo simulations is given by the following reliability analyses:

- i. To estimate the effect of the variability of soil strength parameters on the reliability-based design of bored-pile walls, the probability of failure is defined as $p(\text{Failure} | D/H, \alpha = 0, h_1/H = 1/2)$, with several combinations of the coefficients of variation of friction angle and cohesion. The number of corresponding discrete values of the uncertainty variables is given by $n_{D/H} = 65$, $n_\alpha = 1$ and $n_{h_1/H} = 1$. According to (8), the minimum number of iterations to run in the Monte Carlo simulation is $n_{\min} = 721,500$. The number of realizations considered for this analysis is 7,500,000.
- ii. To determine the influence of the variation of the slope angle of the backfill soil surface on the probabilistic-based design of bored-pile walls, the probability of failure is defined as $p(\text{Failure} | D/H, \alpha, h_1/H = 1/2)$, with $\text{COV}\phi' = 10\%$ and $\text{COV}c' = 30\%$. The number of corresponding discrete values of uncertainty variables is given by $n_{D/H} = 65$, $n_\alpha = 4$, and $n_{h_1/H} = 1$. The minimum number of iterations for the Monte Carlo simulation is

$n_{\min} = 2,886,000$. The number of realizations considered for this analysis is 3,000,000.

- iii. To conduct a parametric analysis of the variation of groundwater level, the probability of failure is defined as $p(\text{Failure} | D/H, \alpha = 0, h_1/H)$ with $\text{COV}\phi' = 10\%$ and $\text{COV}c' = 30\%$. The number of corresponding discrete values of uncertainty variables is given by $n_{D/H} = 65$, $n_\alpha = 1$, and $n_{h_1/H} = 3$.

The minimum number of iterations to run in the Monte Carlo simulation is $n_{\min} = 2,164,500$. The number of realizations considered for this analysis is 2,500,000.

2.2.5 Model parametrization for finite element calculations

To model the soil-structure interaction (SSI) in drained conditions, the two-dimensional finite element code PLAXIS was adopted. The purpose of this finite element analysis (FEA) was to investigate the variations in SSI based on the changes in the groundwater level behind the wall.

The construction sequence of the wall consisted of two stages: initial stage (installation of the wall) and final stage (excavation of the ground in front of the wall up to the dredge level).

The finite element analysis consisted in modeling a 16-m wide excavation using a mesh 46-m wide and 50-m deep. According to Gaba et al. [34], a sensitivity analysis

showed that this mesh resulted in boundaries far enough from the area of interest around the embedded retaining wall that would not influence the results.

The retaining wall was modeled by elastic plate elements to allow an easy extraction of the bending moments.

Interface elements were introduced between the wall and the surrounding soil to allow the control of the interface friction and relative soil/wall movement. Steady-state groundwater seepage pressures were directly computed by the finite element software assuming constant head boundaries at the retained and excavated soil surfaces, an impermeable wall, and zero flow through the vertical line of symmetry [37].

The soil layer was modeled using 15-node triangular elements. This feature of the elements provides a fourth-order interpolation for displacements [38].

The bored-pile wall was modeled using 5-node elastic plate elements. The interface elements had 10 nodes: five on the soil and five on the wall. A typical finite element model mesh for the excavation case consisted of a total of 1513 elements. Due to a stress concentration in and around the wall, a finer finite element

mesh was used in these areas, and the mesh became coarser in the zones far from the bored-pile wall. An elastic-plastic model was used to describe both the soil layer and the soil/structure interface. A linear-elastic model was used to describe plate behavior.

3. RESULTS AND DISCUSSION

Fig. 3 shows the relationship between the probability of failure, given as a conditional probability $p(Failure|D/H, \alpha=0, h_1/H=1/2)$, and the normalized embedment depth (D/H) for several combinations of the coefficient of variation of the friction angle and cohesion. Fig. 3 also includes the $p_T^{SLS} = 1.9 \times 10^{-3}$ value, which was adopted in Eurocode-7 [20].

For a given value of D/H , the probability of failure decreases as D/H increases; this means that the increase in embedment depth leads to greater stability of the wall. Moreover, in terms of feasible normalized embedment depth, the effect of cohesion on the design is significant compared to that of friction angle, as shown in Table 3.

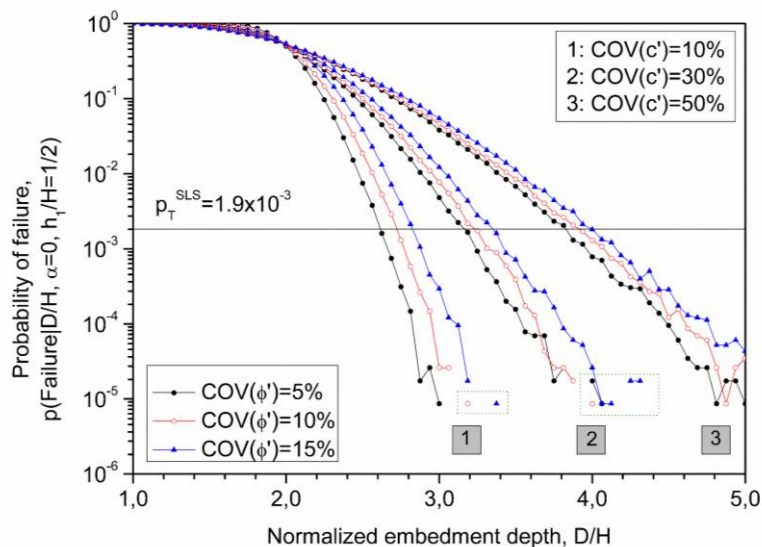


Fig. 3. Effect of soil variability on the reliability-based design of the bored-pile wall
Source: Created by the authors.

Table 3. Feasible and maximum embedment depths based on soil variability
Source: Created by the authors.

D/H _{Feasib}	D/H _{Max}	COV ϕ'	COV c'
2.61	3.00	5 %	10 %
2.72	3.19	10 %	
2.84	3.38	15 %	
3.15	4.06	5 %	30 %
3.23	4.00	10 %	
3.34	4.31	15 %	
3.83	5.00	5 %	50 %
3.90	5.00	10 %	
4.00	5.00	15 %	

The feasible and maximum normalized embedment depths range between 2.61 and 4.0 and 3.0 and 5.0, respectively. The reason why at COV c' =50 % all the maximum embedment depths are identical is that $D/H = 5.0$ is the limit considered in expanded reliability-based designs according to the θ set. Furthermore, the points in the boxes in Fig.3 mean that, at small probability levels (e.g., $p(\text{Failure} | D/H, \alpha=0, h_1/H=1/2) < 7 \times 10^{-4}$), the designs lead to alterations of the embedment depths and, consequently, calculation errors.. Additionally, it can be seen that the choice of the p_T^{SLS} value drastically affects the feasible embedment depth.

These results imply that a great uncertainty in the possible range of variation of the cohesion will also cause a great uncertainty to determine the embedment depth of the bored-pile wall.

A solution to reduce the increasing effect of the uncertainty propagation is to decrease the confidence interval of this variable (e.g., by improving its accuracy through a greater number of measurements).

Fig. 4 shows the influence of the slope angle of the backfill soil on the reliability-based design of the bored-pile wall. The normalized embedment depth increases

considerably as the slope angle increases, while the probability of failure decreases.

The sudden increase of the embedment depth is related to (5), in which the parameter $\cos \alpha$ is squared. Generally speaking, these structures are planned considering the current inclination of the slope or a design slope angle. However, the results show that, for relatively high slopes ($\alpha \geq \sim 10^\circ$ in this case study), a small variation (e.g., increase of the slope by anthropic actions or mass movements) would require a greater embedment depth.

Therefore, the structure initially designed could present instability. In this situation, a retention system already built could not be modified since a greater embedment depth would be required.

Fig. 4 also shows that the number of iterations considered in the Monte Carlo simulations (i.e., 2.5×10^6 realizations) is not enough to obtain an adequate resolution of the reliability-based design results. A low resolution of the normalized embedment depth values for $\alpha \leq 10^\circ$ at $p_T^{\text{SLS}} \leq 1.9 \times 10^{-3}$ is observed. In contrast, Fig. 3 shows a high resolution of the results for $\alpha \leq 10^\circ$ at $p_T^{\text{SLS}} > 7 \times 10^{-4}$ with 7.5×10^6 iterations executed in the simulations. The term *resolution* indicates the degree of alteration of the reliability-based design results: a high resolution of the results means a minor alteration of them.

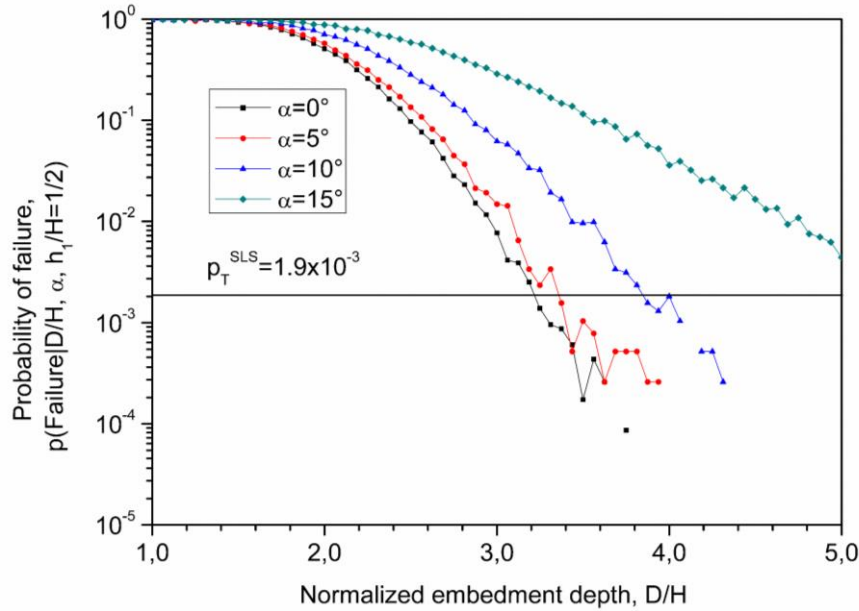


Fig. 4. Influence of the slope angle of the backfill soil surface on the reliability-based design of the bored-pile wall
Source: Created by the authors.

The difference in the number of iterations executed to obtain the reliability-based design results between the reliability analyses 1 and 2 (Fig. 3 and 4) was 4.5×10^6 iterations. This means that the resolution of the results obtained at small probability levels determines the influence of the number of iterations required in the simulations. Other studies [3], [14] recommend multiplying by 10 the minimum number of realizations to run in the Monte Carlo simulation determined through (8) to mitigate the degree of alterations to the reliability-based design results.

Table 4 shows feasible and maximum normalized embedment depth values as a function of the slope angle α . The results indicate that, at $\alpha = 15^\circ$, a normalized embedment depth greater than 5.0 must be considered to calculate both the feasible depth at $p_T^{\text{SLS}} = 1.9 \times 10^{-3}$ and the maximum depth values, although a higher computational cost is required mainly because of the $n_{D/H}$ parameter.

Fig. 5 shows the effect of hydrostatic pressures on the stability of the bored-pile wall according to the reliability-based design approach. The higher the

normalized groundwater level, the greater the feasible normalized embedment depth, while the probability of failure decreases, as shown in Table 5. The increase in the groundwater level occurs linearly according to (2), and (4), which are first-degree polynomials. Although this probabilistic result is derived from an uncertainty model, the deterministic component is significant; basically, this happens because, in the uncertainty model, a discrete uniform distribution is considered to model the groundwater level.

After this assessment, we considered appropriate to extend the study of the effects of the groundwater level on the wall stability through a soil-structure interaction analysis using the finite element method.

In this study, finite element calculations were executed considering the most critical design condition based on Fig. 5, that is, when the normalized groundwater level is at the retained ground surface (i.e., $h_1/H=0$). Table 5 indicates that $D/H_{\text{Feasib}} = 3.73$ at $h_1/H = 0$; therefore, the feasible embedment depth is $D_{\text{Feasib}} = 14.92 \text{ m} \approx 15 \text{ m}$.

Table 4. Feasible and maximum embedment depths at different slope angles of the retained ground surface. Source: Created by the authors.

Slope angle	$\alpha=0^\circ$	$\alpha=5^\circ$	$\alpha=10^\circ$	$\alpha=15^\circ$
D/H_{Feasib}	3.23	3.35	3.85 and 3.99*	unknown
D/H_{Max}	3.75	3.94	4.31	unknown

Table 5. Feasible and maximum embedment depths at different groundwater levels
Source: Created by the authors.

G.W.L.	$h_1/H=0$	$h_1/H=1/2$	$h_1/H=1$
D/H_{Feasib}	3.73	3.23	2.71
D/H_{Max}	4.44	4.00	3.25

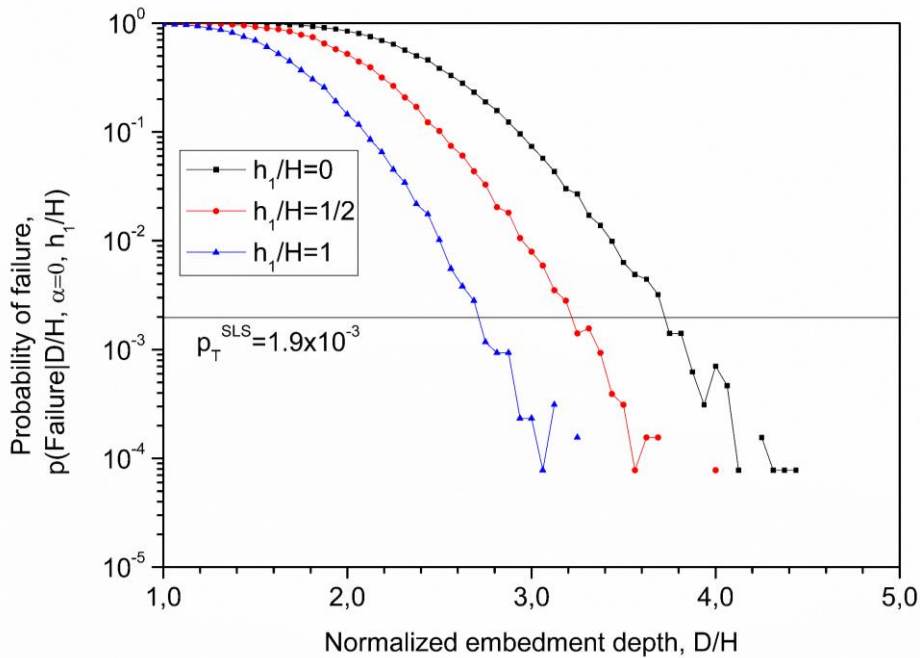


Fig. 5. Effect of the groundwater level on the reliability-based design of the bored-pile wall
Source: Created by the authors.

Fig. 6a and 6b show the bending moments and shear forces of the wall based on the normalized groundwater level changes. The maximum value of the bending moment and the shear force increase suddenly as the normalized groundwater level rises from $\frac{1}{2}$ to 1.

This result is derived from the groundwater flow calculation performed to generate the pore pressure distribution.

Fig. 7 shows the wall movements caused by changes in the normalized

groundwater level obtained from the finite element analysis using PLAXIS.

With the groundwater at the dredge level (i.e., $h_1/H = 1$), the upper end of the wall moves 5.3 mm away from the retained soil, unlike the lower end, which moves 0.7 mm less. On the other hand, when the groundwater level is at $h_1/H = 1/2$, the upper end of the wall moves 7.8 mm away from the retained soil, while the lower end moves 6.2 mm. Furthermore, the point with the least displacement in the wall

($\delta_x=5.4$ mm) is 8.27 m below the surface of the retained soil. Finally, when the groundwater level is located at the retained ground surface (i.e., $h_1/H=0$), the horizontal displacement of the upper end of the wall reaches 15.2 mm, approximately 0.0038 times the free height of the wall.

This design condition slightly meets the design specifications given by NSR-10, in which, for the serviceability limit state, the maximum horizontal displacement of the

upper end of the wall must be $0.001 H \leq \delta_x \leq 0.004 H$ for coarse-grained soils in an active stress state.

The results show that the depth of the water table has a great influence on the stability of the retaining wall. For this reason, the design of these structures should consider the least probable scenarios of the groundwater level that could occur, although levels are above what is shown in the field explorations.

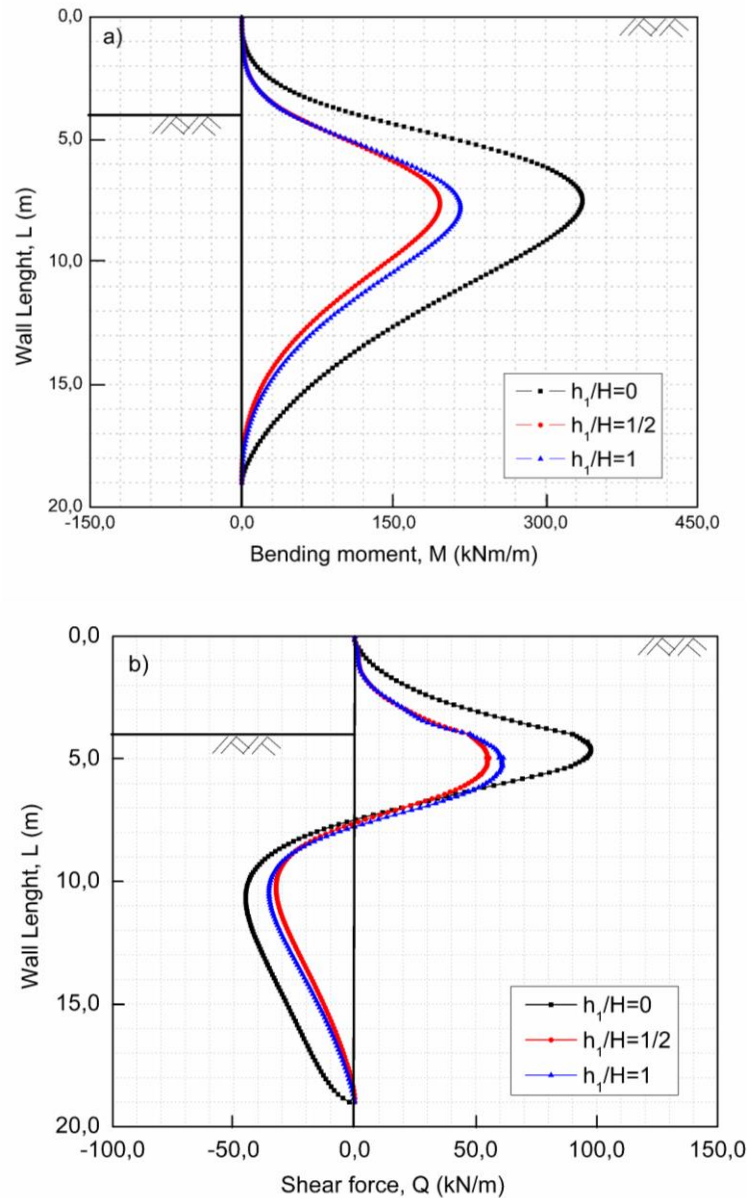


Fig. 6. Groundwater level changes reflected in (a) bending moments and (b) shear forces
Source: Created by the authors.

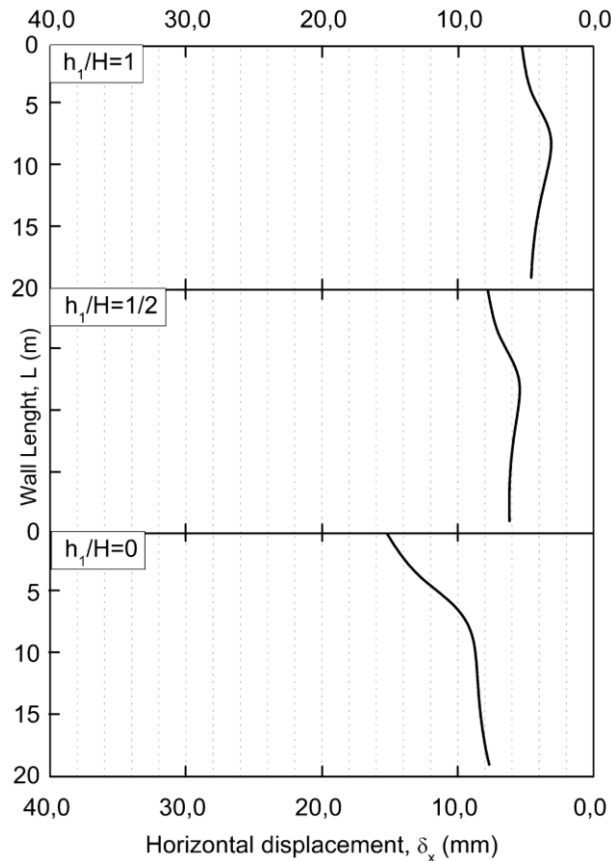


Fig. 7. Wall deflection magnitudes caused by groundwater level changes
Source: Created by the authors.

An increase in the water table above an assumed scenario based on field measurements could cause unacceptable deformations or affect the instability since the embedment depth of the bored-pile wall would not be enough.

The reliability-based design methodology implemented for a bored-pile wall has the advantage of considering different distinctive elements (e.g., correlated load and resistance and multiple correlated failure modes). Nevertheless, direct Monte Carlo approaches are sometimes criticized because of a lack of computational efficiency and resolution at small probability levels (e.g., feasible domains with the probability of failure less than the target probability of failure).

Extensive computational efforts are required when a series of scenarios are of interest in geotechnical design.; hence,

repeated MCS-based probabilistic analyses are needed to re-design the geotechnical structure. However, the number of new applications for geotechnical reliability-based design of retaining structures is increasing due to the development of computer technologies [5].

Besides the quantitative incorporation of the uncertainty parameter in the analysis, another great advantage of the stochastic method implemented here is the possibility of analyzing different scenarios.

The latter include critical or less probable conditions (e.g., groundwater level at the retained ground surface), in contrast to the most probable conditions (using the average values of geotechnical parameters) [39].

4. CONCLUSIONS

We conducted parametric analyses of bored-pile wall stability. They showed that the soil variability, groundwater level, and slope angle of the retaining ground surface are factors that affect the embedment depth of the wall, especially cohesion, whose influence on stability is derived from the fact that the degree of uncertainty is usually higher than that of the other geotechnical parameters. In this case, we found that a great uncertainty in the coefficient of variation of cohesion will affect the calculation of the embedment depth of the bored-pile wall.

The reliability-based design approach is a powerful method for exploration purposes and uncertainty analysis of geotechnical design parameters; however, it requires running a high number of iterations to reach an appropriate resolution in the results. Additionally, finite element analysis is considered an adequate complementary method for it, fundamentally in the parametric analysis of the groundwater level.

The soil-structure interaction analysis implementing the finite element method demonstrated that, at different heights of the groundwater level, a severe rotation of the upper end of the wall was caused, along with a progressive horizontal displacement of the lower end, which was much shorter but equally important for the serviceability limit state according to the NSR-10 standard.

5. CONFLICTS OF INTEREST

The authors declare that they have no conflict of interest.



6. REFERENCES

- [1] Asociación Colombiana de Ingeniería Sísmica (AIS), “Reglamento Colombiano de Construcción Sísmo Resistente (NSR-10).”
- [2] Ministerio de Ambiente, Vivienda y Desarrollo Territorial, Bogotá, D.C., Colombia, 2010. Disponible en: URL
- [3] D.-Q. Li, K.-B. Shao, Z.-J. Cao, X.-S. Tang, and K.-K. Phoon, “A generalized surrogate response aided-subset simulation approach for efficient geotechnical reliability-based design,” *Comput. Geotech.*, vol. 74, pp. 88–101, Apr. 2016. <https://doi.org/10.1016/j.compgeo.2015.12.010>
- [4] Y. Wang, “MCS-based probabilistic design of embedded sheet pile walls,” *Georisk*, vol. 7, no. 3, pp.151–162, Mar. 2013. <https://doi.org/10.1080/17499518.2013.765286>
- [5] R. J. Bathurst, P. Lin, and T. Allen, “Reliability-based design of internal limit states for mechanically stabilized earth walls using geosynthetic reinforcement,” *Can. Geotech. J.*, vol. 56, no. 6, pp. 774–788, Jun. 2019. <https://doi.org/10.1139/cgj-2018-0074>
- [6] Z.-J. Cao, X. Peng, D.-Q. Li, and X.-S. Tang, “Full probabilistic geotechnical design under various design scenarios using direct Monte Carlo simulation and sample reweighting,” *Eng. Geol.*, vol. 248, no. 8, pp. 207–219, Jan. 2019. <https://doi.org/10.1016/j.enggeo.2018.11.017>
- [7] E. F. García-Aristizábal, E. V. Aristizabal-Giraldo, R. J. Marín Sánchez, and J. C. Guzman-Martinez, “Implementación del modelo TRIGRS con análisis de confiabilidad para la evaluación de la amenaza a movimientos en masa superficiales detonados por lluvia,” *TecnoLógicas*, vol. 22, no. 44, pp. 111–129, Jan. 2019. <https://doi.org/10.22430/22565337.1037>
- [8] Z. Q. Xiao, J. Huan, Y. J. Y. Wang, C. Xu, and H. Xia, “Random Reliability Analysis of Gravity Retaining Wall Structural System,” in *2014 International Conference on Mechanics and Civil Engineering (icmce-14)*, Dec. 2014. <https://doi.org/10.2991/icmce-14.2014.36>
- [9] B. Hu, Z. Luo, C. L. Ho, and Y. Wang, “Efficient Reliability-Based Design Tool for Reinforced Earth Retaining Walls of Heavy Haul Railway Considering Internal Failure Modes,” in *2018 Joint Rail Conference*, Pennsylvania, 2018. <https://doi.org/10.1115/JRC2018-6110>
- [10] P. Zeng, T. Li, R. Jimenez, X. Feng, and Y. Chen, “Extension of quasi-Newton approximation-based SORM for series system reliability analysis of geotechnical problems,” *Eng. Comput.*, vol. 34, no. 2, pp. 215–224, Aug. 2018. <https://doi.org/10.1007/s00366-017-0536-8>
- [10] R. J. Marín, J. C. Guzmán-Martínez, H. E. Martínez Carvajal, E. F. García-Aristizábal,

- J. D. Cadavid-Arango, and P. Agudelo-Vallejo, "Evaluación del riesgo de deslizamientos superficiales para proyectos de infraestructura: caso de análisis en vereda El Cabuyal," *Ing. y Cienc.*, vol. 14, no. 27, pp. 153–177, Jun. 2018.
<https://doi.org/10.17230/ingciencia.14.27.7>
- [11] G.-H. Gao, D.-Q. Li, Z.-J. Cao, Y. Wang, and L. Zhang, "Full probabilistic design of earth retaining structures using generalized subset simulation," *Comput. Geotech.*, vol. 112, pp. 159–172, Aug. 2019.
<https://doi.org/10.1016/j.compgeo.2019.04.020>
- [12] W. Dong, "A Reliability Study of a Retaining Wall Design with Seismic Loads," in *Geo-Congress 2020: Engineering, Monitoring, and Management of Geotechnical Infrastructure*, Minneapolis, 2020, pp. 543–551.
<https://doi.org/10.1061/9780784482797.052>
- [13] K. K. Phoon and J. Ching, "Semi-probabilistic reliability-based design," in *Reliability of Geotechnical Structures in ISO2394*, K. K. Phoon and J. V. Retief, Eds. London: CRC Press, 2016, pp. 160–192.
- [14] Y. Wang, T. Schweckendiek, W. Gong, T. Zhao, and K.-K. Phoon, "Direct probability-based design methods," in *Reliability of Geotechnical Structures in ISO2394*, K.K. Phoon & J.V. Retief, Ed. London: CRC Press, 2016, pp. 194–226. Disponible en: <URL>
- [15] K. K. Phoon, F. H. Kulhawy, and M. D. Grigoriu, "Reliability-based design for transmission line structure foundations," *Comput. Geotech.*, vol. 26, no. 3–4, pp. 169–185, Apr. 2000.
[https://doi.org/10.1016/S0266352X\(99\)00037-3](https://doi.org/10.1016/S0266352X(99)00037-3)
- [16] J. C. Viviescas, J. P. Osorio, and J. E. Cañón, "Reliability-based designs procedure of earth retaining walls in geotechnical engineering," *Obras y Proy.*, no. 22, pp. 50–60, Dec. 2017.
<http://dx.doi.org/10.4067/S071828132017000200050>
- [17] Z. J. Cao, Y. Wang, D. Li "Practical reliability analysis and design by Monte Carlo Simulation in spreadsheet," in *Risk and reliability in geotechnical engineering*, K.-K. Phoon and J. Ching, Eds. London: CRC Press, 2014, pp. 301–335.
https://doi.org/10.1007/978-3-662-52914-0_7
- [18] G. B. Baecher and J. T. Christian, *Reliability and statistics in geotechnical engineering*. John Wiley & Sons Ltd, 2003.
- [19] International Organization for Standardization, "ISO2394:2015. General Principles on Reliability for Structures." Geneva, 2015. Available: <URL>
- [20] CEN, "Eurocode 7 Geotechnical design. Part 1: General rules. EN1997:2004." European Committee for Standardization, Brussels, 2004. Available: <URL>
- [21] B. K. Low and K. K. Phoon, "Reliability-based design and its complementary role to Eurocode 7 design approach," *Comput. Geotech.*, vol. 65, pp. 30–44, Apr. 2015.
<https://doi.org/10.1016/j.compgeo.2014.11.011>
- [22] K. K. Phoon and J. V. Retief, *Reliability of geotechnical structures in ISO2394*. London, UK.: CRC Press, 2016.
- [23] K. K. Phoon, "Role of reliability calculations in geotechnical design," *Georisk*, vol. 11, no. 1, pp. 4–21, Dec. 2016.
<https://doi.org/10.1080/17499518.2016.1265653>
- [24] Asociación Colombiana de Ingeniería Sísmica (AIS), "Norma colombiana de diseño de puentes (CCP-14)." INVIAS, Bogotá, D.C., Colombia, 2014. Available: <URL>
- [25] A. V. D. Bica and C. R. I. Clayton, "Limit equilibrium design methods for free embedded cantilever walls in granular soils," *Proc. Inst. Civ. Engrs.*, vol. 86, pp. 879–898, Oct. 1989. Available: <URL>
- [26] B. J. Hansen, "Earth pressure and water pressure" in *Part II Actions And material Strength*, The institution of danish civil engineers: Copenhagen, 1953. Available: <URL>
- [27] V. N. S. Murthy, *Geotechnical engineering: principles and practices of soil mechanics and foundation engineering*. New York: Marcel Dekker, Inc, 2002.
- [28] Z. H. Mazindrani and M. H. Ganjali, "Lateral Earth Pressure Problem of Cohesive Backfill with Inclined Surface," *J. Geotech. Geoenvironmental Eng.*, vol. 123, no. 2, pp. 110–112, Feb. 1997.
[https://doi.org/10.1061/\(ASCE\)1090-0241\(1997\)123:2\(110\)](https://doi.org/10.1061/(ASCE)1090-0241(1997)123:2(110))
- [29] Y. Wang, "Reliability-based design of spread foundations by Monte Carlo simulations," *Géotechnique*, vol. 61, no. 8, pp. 677–685, Aug. 2011.
<https://doi.org/10.1680/geot.10.P.016>
- [30] Y. Wang, S. K. Au, and F. H. Kulhawy, "Expanded Reliability-Based Design Approach for Drilled Shafts," *J. Geotech. Geoenvironmental Eng.*, vol. 137, no. 2, pp. 40–150, Jan. 2011.
[https://doi.org/10.1061/\(ASCE\)GT.1943-5606.0000421](https://doi.org/10.1061/(ASCE)GT.1943-5606.0000421)
- [31] Z.-J. Cao and Y. Wang, "Practical Reliability-based Design of Deep Foundations Using Subset Simulation," in *Second International Conference on Vulnerability and Risk Analysis and Management (ICVRAM) and the Sixth International Symposium on Uncertainty, Modeling, and Analysis (ISUMA)*, Liverpool, 2014, pp. 2032–2042.
<https://doi.org/10.1061/9780784413609.204>
- [32] A. H.-S. Ang and W. H. Tang, *Probability*
- [178] TecnoLógicas, ISSN-p 0123-7799 / ISSN-e 2256-5337, Vol. 23, No. 48, mayo-agosto de 2020, pp. 163-179

- Concepts in Engineering: Emphasis on Applications in Civil & Environmental Engineering*, 2nd ed. New York: Wiley, 2007.
- [33] R. J. Marin and Á. J. Mattos, “Physically-based landslide susceptibility analysis using Monte Carlo simulation in a tropical mountain basin,” *Georisk Assess. Manag. Risk Eng. Syst. Geohazards*, pp. 1–14, Jun. 2019. <https://doi.org/10.1080/17499518.2019.1633582>
- [34] A. Gaba, S. Hardy, L. Doughty, W. Powrie, and D. Selemetas, *Guidance on embedded retaining wall design (CIRIA Report C760)*. London: CIRIA, 2017.
- [35] K. K. Phoon, *Reliability-based design in geotechnical engineering: computations and applications*. CRC Press, 2008.
- [36] K. K. Phoon and J. Ching, *Risk and reliability in geotechnical engineering*. CRC Press, 2017.
- [37] A. Gaba, B. Simpson, W. Powrie, and D. Breadman, *Embedded retaining walls: guidance for economical design (CIRIA Report C580)*. London: CIRIA, 2003.
- [38] Ö. Bilgin, “Numerical studies of anchored sheet pile wall behavior constructed in cut and fill conditions,” *Comput. Geotech.*, vol. 37, no. 3, pp. 399–407, Apr. 2010. <https://doi.org/10.1016/j.compgeo.2010.01.002>
- [39] Á. J. Mattos, “Reliability analysis of cantilever bored-pile walls,” (Master’s Thesis) University of Antioquia. 2019. Available: [URL](#)

7. AUTHOR CONTRIBUTIONS

- ¹ Directed the research project and chose the models and methods implemented. He determined the methodology, made the calculations, and prepared the figures and tables. He worked actively (leading) in the different sections of the research article.
- ² Worked in the analysis of the results, discussion, and conclusions. He revised the manuscript, corrected the writing style, and improved the article in the different sections.